

**Al, Ti, and Cr: Complex zoning in synthetic and natural nakhlite pyroxenes.** G. McKay<sup>1</sup>, L. Le<sup>2</sup>, and T. Mikouchi<sup>3</sup>, <sup>1</sup>Mail Code KR, NASA Johnson Space Center, Houston, TX 77058, <sup>2</sup>ESC Group, NASA Johnson Space Center, <sup>3</sup>Dept. of Earth and Planetary Science, Univ. of Tokyo, 7-3-1 Hongo, Tokyo 113-0033, Japan.

**Introduction:** Nakhrites are olivine-bearing clinopyroxene cumulates [e.g., 1]. The cumulus pyroxenes have cores that are relatively homogeneous in Fe, Mg, and Ca, but show complex zoning of minor elements, especially Al, Ti, and Cr. Zoning patterns contain information about crystallization history parent magma compositions. But it has proven difficult to decipher this information and translate the zoning patterns into petrogenetic processes [2-5]. This abstract reports results of high-precision EPMA analysis of synthetic nakhlite pyroxenes run at  $fO_2$  from IW to QFM. It compares these with concurrent analyses of natural nakhlite MIL03346 (MIL), and with standard-precision analyses of Y000593 (Y593) collected earlier. Results suggest that (1) different processes are responsible for the zoning of MIL and other more slowly-cooled nakhrites such as Y593, and (2) changes in oxidation conditions during MIL crystallization are not responsible for the unusual Cr zoning pattern [4].

**Analyses:** Individual elements were counted for sufficient time to yield 1-sigma counting statistics of better than  $\pm 0.16$  wt% for Si and Ca, 0.10% for Fe, .06 for Mg, and .02 for all other elements. Analyses were performed on MIL and four synthetic samples using a single standardization. All samples were carbon-coated at the same time. These procedures result in minimum bias between samples so that all can be directly compared.

**Results:** Fig. 1 shows element maps of pyroxenes from Y593 and MIL. Al and Ti display patchy zoning in Y593, and show only very minor zoning of Cr. In contrast, MIL pyroxenes show almost no zoning in Al (not shown), but significant zoning of Cr. The latter tends to be depleted in the centers of the crystals and enriched in the outer portions of the homogeneous cores. Fig 2. shows a BSE image and an Al map of a

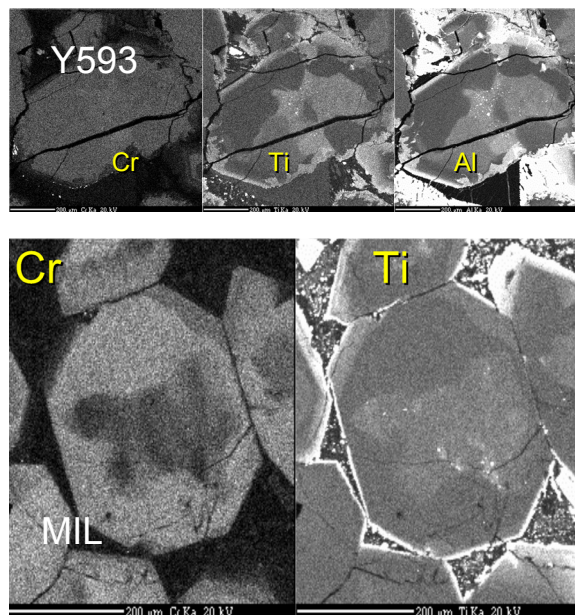


Fig. 1. Maps of Cr, Ti, and Al zoning in Nakhlite pyroxenes. Each image is  $\sim 500$   $\mu\text{m}$  across.

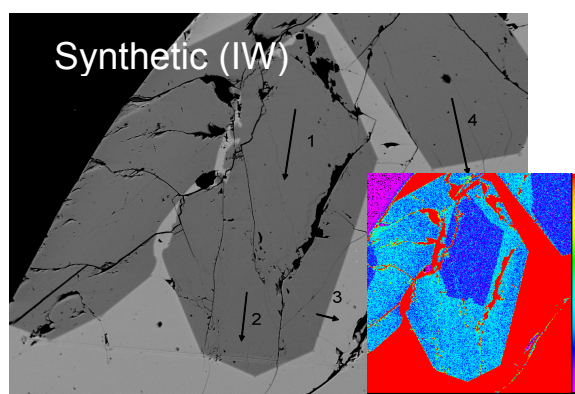


Fig. 2. BSE image and Al map (inset) of synthetic pyroxene grown at IW. Analytical traverses are marked on BSE image. Map  $\sim 600$   $\mu\text{m}$  across.

synthetic nakhlite pyroxene that crystallized at IW. Al-poor regions in the center of the large grain and bottom of the top right grain were produced by sector zoning.

Variation of Cr with Ti is shown in Fig. 3 for synthetic pyroxenes crystallized at four oxygen fugacities, and for MIL pyroxene cores. Routine (less precise) analyses of Y593 pyroxenes are also shown. Note Cr decreases with increasing Ti for MIL, in contrast to all other samples. Fig 4 shows variation of Cr with Fe/Mg. Again, in con-

trast to all other samples, Cr in MIL decreases with increasing Fe/Mg. These trends suggest fractional crystallization played a part in MIL pyroxenes. Cr is highly compatible in pyroxene, and would be strongly depleted from the melt during fractional crystallization. However, the fact that most Cr-poor regions are in the center of grains would require that these grains initially formed as hollow skeletons, or hopper grains, and subsequently filled in as Cr was depleted from the melt. There is no suggestion of this behavior in other nakhlites, which do not show the low Cr contents displayed by the MIL central pyroxenes.

Fig 5. shows structural formula data calculated from microprobe analyses and sheds light on substitution mechanisms for alter-valent cations in these nakhlite pyroxenes. A perfect analysis in which all Al is in the tetrahedral site and is charge compensated by Ti or Cr would plot along the line of slope 1. All pyroxenes plot below that line, indicating either that some Cr or Ti is entering as reduced species, or else some of the Al is entering the octahedral sites. Lack of correlation with  $fO_2$  for the synthetic charges renders the former unlikely. This result suggests that Al activity was higher or Si activity lower in the melt from which MIL crystallized.

Because  $D(Cr)$  in our experiments is a strong function of  $fO_2$ , we investigated the possibility that changes in redox conditions could be responsible for variations in MIL Cr. MELTS calculations indicate that the cation total calculated from EPMA analyses (Fig. 6) would increase with  $fO_2$ . The magnitude of the expected increase is indicated by the bar at the right in Fig. 6. Although we see an increase in cation total from IW to QFM pyroxenes, there is no significant difference in cation total between Cr-rich and Cr-poor regions of MIL pyroxene. Thus it appears that redox changes are not responsible for the observed Cr variations.

**References:** [1] Treiman, A. (2005) *Chem Erde* 65, 203. [2] McKay & Mikouchi (2005) *MAPS* 40, A5335. [3] McKay *et al.* (2006) *Antarctic Meteorites* 30, 61. [4] McKay *et al.* (2007) *LPSC* 38, 1721. [5] Cameron & Papike (1981) *Am. Min* 66, 1.

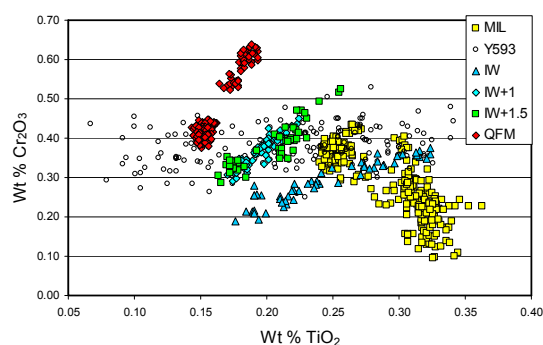


Fig. 3. Variation of Cr with Ti for synthetic pyroxenes from IW to QFM and for MIL. Less precise analyses of Y593 are also shown.

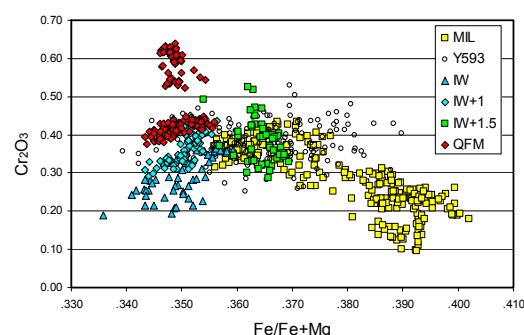


Fig 4. Variation of Cr with Fe/Mg for synthetic pyroxenes, MIL, and Y593.

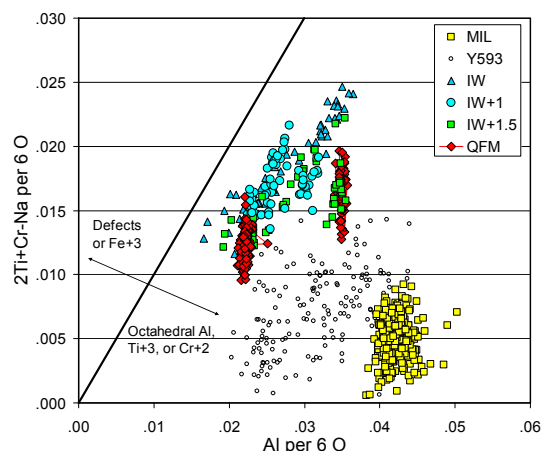


Fig. 5. Structural formula calculation indicating substitution mechanisms for Ti and Al [5].

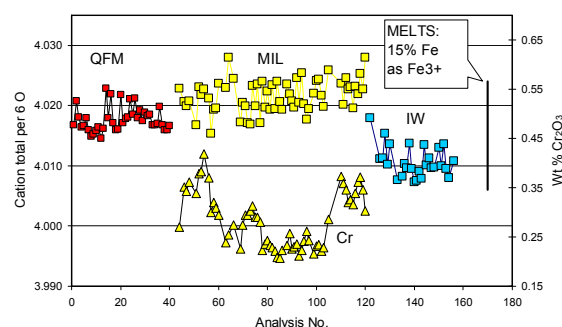


Fig. 6. Cation totals for synthetic and Mil pyroxenes. Cr profile is shown to indicate location of Cr-rich outer regions. Bar at right shows predicted change in cation total from IW (bottom) to QFM (top).